Chemical Engineering Journal 107 (2005) 103–111

Chemical Engineering Journal

www.elsevier.com/locate/cej

Theoretical studies on multifunctional catalysts with integrated adsorption sites

Wulf Dietrich*, Praveen S. Lawrence, Marcus Grünewald, David W. Agar

Department of Biochemical and Chemical Engineering, University of Dortmund, Emil-Figge-Str. 66, D-44227 Dortmund, Germany

Abstract

Adsorptive reactors represent a promising application of the multifunctional reactor concept for process intensification. The deliberate manipulation of concentration and temperature profiles resulting from the integration of an additional adsorptive functionality with heterogeneous catalytic activity can be impeded significantly by mass transfer limitations. If the multifunctionality is extended down to the particle level by using a multifunctional catalyst design the mass transfer bottleneck can be circumvented. Structured multifunctional catalyst particles offer an additional degree of freedom in reactor design. The enhancement in performance from multifunctional catalysts with integrated adsorption sites was evaluated for two reaction systems of industrial relevance using a rigorous dynamic model. Significant improvements were found when mass transfer limitations were present and a simple design procedure is presented for selecting the optimal particle structure of multifunctional catalysts.

Keywords: Process intensification; Multifunctional catalysts; Non-uniform activity distribution; Adsorptive reactors

1. Introduction

The integration of multiple process functions in multifunctional reactors, e.g. through the combination of heterogeneous catalytic reactions and separation processes, has been studied extensively over the last few years as a promising means of process intensification [1]. Apart from the better known processes of reactive distillation, membrane reactors and chromatographic reactors the potential available through the integration of an additional unit operation into a chemical reactor has been demonstrated for the concept of adsorptive reactors in a variety of interesting applications, e.g. Claus process [2], steam reforming [3–5], methanol-synthesis [6,7], dehydrogenations [8,9]. Generally, the incorporation of an adsorptive functionality is a particularly effective means of deliberately manipulating concentration profiles in an expedient manner. In the case of an integrated adsorptive removal of a reaction (by-)product an enhanced conversion for equilibrium limited reactions can be achieved. Similarly, unwanted consecutive reactions can be suppressed improving selectivity if the desired intermediate is removed by adsorption.

Whenever more than one functionality is to be incorporated into a reactor the spatial distribution of the functionalities can be exploited as an additional design parameter to optimise reactor performance. So far the structured distribution of individual functionalities within adsorptive reactors has been carried out solely on the reactor scale, e.g. by the non-uniform spatial distribution of adsorbent and catalyst particles along a fixed-bed [10].

However, the inter- and intra-particle mass transfer can impose a serious constraint on the utilisation of the synergy potential offered by adsorptive reactors, since the manipulation of concentration profiles depends strongly on the mass transfer between the two functionalities. This fact is reflected in the strict criteria for compatible reaction and adsorption rates if the application of adsorptive reactors is to be feasible [2]. If the functionalities are integrated at the particle level, an intensification of the mass transfer between the various functional sites can be expected.

Furthermore, microstructuring offers an additional degree of freedom in the design of a multifunctional reactor, since the functionalities can be expediently structured within the

* Corresponding author. Tel.: +49 231 755 4347; fax: +49 231 755 2698.
E-mail address: wulf.dietrich@bci.uni-dortmund.de (W. Dietrich).

1385-8947/$ – see front matter © 2004 Elsevier B.V. All rights reserved.
doi:10.1016/j.cej.2004.12.016

Nomenclature

c_i	bulk phase concentration (mol/m^3)
$c_{p,i}$	particle concentration (mol/m^3)
$c_{0,i}$	reactor inlet concentration (mol/m^3)
D_{ax}	axial dispersion coefficient (m^2/s)
$D_{eff,i}$	effective pore diffusion coefficient $D_{eff,i} = D_i\varepsilon/\tau$ (m^2/s)
D_i	molecular diffusion coefficient (m^2/s)
$f_{p,ads}$	adsorbent volume fraction of multifunctional particle
$f_{p,cat}$	catalyst volume fraction of multifunctional particle
$f_{x,ads}$	adsorbent particle fraction in conventional reactor
$f_{x,cat}$	catalyst particle fraction in conventional reactor
k	rate constant, water–gas shift reaction (mol/bar^2 m^3 s)
$k_{eff,i}$	effective mass transfer coefficient (m/s)
$k_{film,i}$	external particle mass transfer coefficient (m/s)
k_1	forward reaction rate constant, Claus reaction (mol/bar$^{1.25}$ m^3 s)
k_2	reverse reaction rate constant, Claus reaction (mol/bar m^3 s)
K_{eq}	equilibrium constant, water–gas shift reaction
$K_{F,i}$	Freundlich constant ((mol/m^3)$^{0.25}$)
K_i	Langmuir constant, water–gas shift reaction (bar^{-1})
L	reactor length (m)
p_i	partial pressure (bar)
q_i	adsorbent loading (mol/m^3)
r	radial coordinate (m)
$r_{V,ads,i}$	adsorption rate (mol/m^3 s)
$r_{V,cat,i}$	reaction rate (mol/m^3 s)
R_p	particle radius (m)
St	Stanton number
t	time
t_{cyc}	cycle time (s)
Δt_{rel}	relative cycle time enhancement (%)
u	superficial gas velocity (m/s)
V_p	particle volume (m^3)
x	axial coordinate (m)
X	conversion

Greek letters

ε	reactor void fraction
ε_p	particle porosity
Φ	Thiele modulus
ν	stochiometric coefficient
τ	particle tortuosity factor

Subscripts

ads	adsorbent particle
cat	catalyst particle
hom	multifunctional particle with homogenous (uniform) structure
opt	multifunctional particle with optimal structure

particles thus providing a tool for the direct manipulation of intra-particle concentration and temperature profiles. The deliberate exploitation of adsorption phenomena in heterogeneous catalyst is by no means an unknown concept, and has been utilised previously in automotive exhaust catalysis, for instance, to maintain suitable oxygen levels in three-way catalysts or to remove nitrogen oxides from diesel exhausts through periodic lean-rich operation.

In this work the potential of multifunctional catalysts with integrated adsorption sites is evaluated in comparison to the corresponding 'conventional' adsorptive reactor configuration. Model parameter studies have been carried out using an appropriate dynamic simulation for two equilibrium reactions in order to identify the areas in which multifunctional catalysts might be used to advantage and to quantify the attainable gains in reactor performance.

2. Multifunctional adsorptive catalysts

Under certain conditions, i.e. in the case of fast reactions or low intra-particle mass transfer rates, the potential synergy offered by the integration of an additional adsorptive functionality in a multifunctional reactor is diminished by mass transfer limitations and thus lack of driving force. If the principle of multifunctionality is extended down to the particle level a more intimate spatial integration of the functionalities can be achieved. The decreased distance between the different functional sites results in an intensification of the intra-particle mass transfer and thus offers a more direct and effective manipulation of the intra-particle concentration profiles.

In the case of conversion enhancement for an equilibrium-limited reaction via adsorptive product removal, the benefits provided by multifunctional catalysts can be easily illustrated as depicted in Fig. 1. For a simple bimolecular equilibrium reaction the thermodynamic equilibrium is shifted towards the product side according to Le Chatelier's principle if the reaction (by-)product C is adsorbed.

In a multifunctional particle the component C can be adsorbed directly in the same particle in which it is formed, while in a 'conventional' arrangement C has to be transported from the catalyst particle via the bulk fluid phase into a neighbouring adsorbent particle. As a result a lower concentration of the product is achieved at the catalyst surface yielding a higher rate of reaction compared to a simple monofunctional catalyst particle. The more direct local product removal also results in an increased driving force for the adsorption process and thus better utilisation of the adsorbent capacity. In

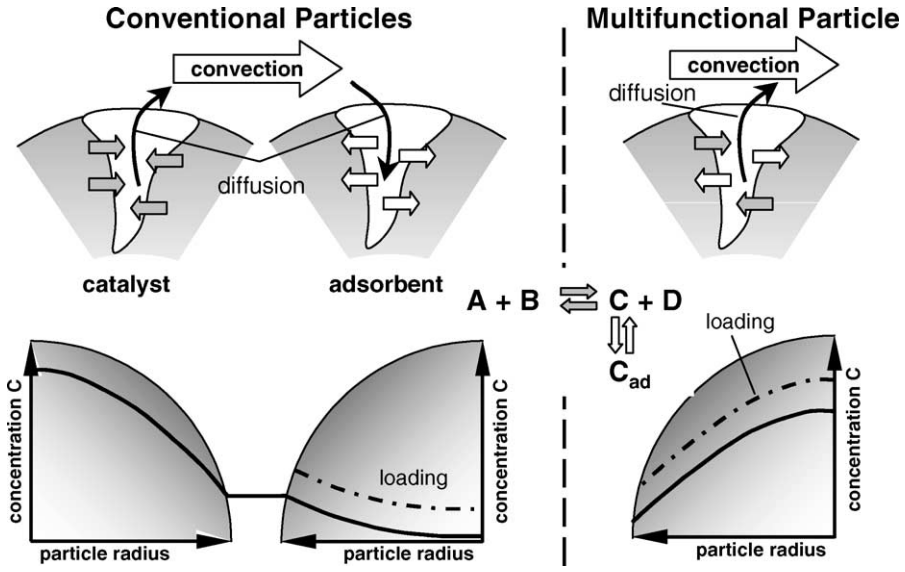

Fig. 1. Schematic comparison of the coupling of reaction and adsorption and the resulting concentration profiles for conventional and multifunctional particles.

addition the bulk phase concentration of C is diminished, so that the integrated functionalities at the particle scale lead to steeper concentration profiles in the reactor and therefore yield sharper breakthrough curves for both the adsorbed component and unconverted reactants permitting longer cycle times in adsorptive reactor operation. For a given reactor volume and reactant flow rate an extended cycle time is equivalent to a higher space–time-yield.

The integration of two different catalytic functionalities within bifunctional particles and the influence of the intraparticle distribution of the catalytic activities on reactor performance was investigated as early as in the 1960s and 1970s [11,12]. However, the deliberate integration of adsorptive and catalytic functionalities in a single particle has so far attracted little attention. Only the use of bifunctional catalytic materials serving as both adsorbent and catalyst has been reported in a few instances. For example, esterification reactions in a liquid chromatographic reactor using the ion exchange resins both as adsorbent and catalyst were investigated by Kawase et al. [13] and Silva and Rodrigues [14]. In this contribution we focus more generally on catalyst systems consisting of distinct functionalities, which can be structured in an expedient manner within a ‘catalyst’ particle.

Microscale distribution is hardly an entirely new approach in chemical engineering [15]. The non-uniform distribution of the adsorptive and catalytic functionalities inside a multifunctional particle promises an additional degree of freedom in the design and optimisation of adsorptive reactors. Both the composition, i.e. the overall fraction of each ‘activity’, and the spatial distribution of the individual activities at the particle and reactor level become available as additional design parameters.

The optimal distribution of a single and two different catalytic activities in a particle has been investigated previously under steady-state conditions. For a single catalytic activity the optimal particle structure, i.e. the relative location of the

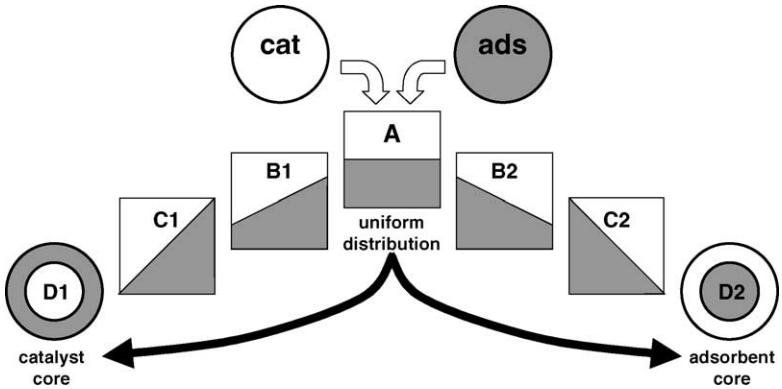

Fig. 2. Selection of structure variants considered in the optimisation of the particle microstructure.

activity within the particle, is determined by the reaction kinetics as well as by the mass transfer rate of the reactants. For certain reaction kinetics, analytical solutions of the optimisation problem can be derived [15]. For the combination of two different catalytic activities catalysing different reactions in a multi-step synthesis within a single particle it has been demonstrated that an optimisation of the activity profiles allows a significant increase in both overall reaction rate and selectivity [16]. In contrast to these "steady-state" studies the emphasis in our own research is on multifunctional catalysts with integrated adsorption sites for the conversion enhancement of equilibrium limited reversible reactions. Due to the inherent unsteady-state nature of adsorption processes, the theoretical analysis of these multifunctional catalysts has to be carried out under transient conditions.

Based on the dynamic simulation model developed in this work, the structure of such multifunctional catalysts has been optimised by following a simplified iterative procedure. A discrete set of particle structures (Fig. 2) was selected a priori to provide a representative spectrum of possible arrangements for two different functionalities and taking the manufacturing feasibility for such particles into consideration. Proceeding from the highest degree of integration – a homogenous or uniform mixture of adsorptive and catalytic functionalities – the volume fractions have been separated progressively and discretely until core-shell arrangements are attained (Fig. 2).

3. Modelling

A two phase dispersion model with internal pore diffusion describing the dynamic behaviour of a fixed-bed adsorptive reactor with multifunctional catalyst as well as for a benchmark with separate catalyst and adsorbent particles has been developed. The spatial distribution of the functionalities within the multifunctional catalyst particles was described according to the volume fraction of each functionality, whereby all possible particle structures could be accounted for. The model development was based on the following general assumptions:

- the contribution of adsorption and reaction to the particle mass balance can be described by the relative volume fractions of each functionality which are a function of the radial position,
- the fluid in the particle pores and the internal adsorbent and catalyst surface is in equilibrium,
- the adsorption process was assumed to be only mass transfer limited,
- the physical structure of the particles can be idealised as porous spheres with a uniform pore structure independent of the functionality distribution,
- particle size and structure were averaged for all particles (multifunctional and conventional) in order to permit a direct comparison of different particle and reactor configurations,
- a non-ideal plug flow of the bulk fluid phase is assumed with axial backmixing being lumped in an axial dispersion coefficient,
- the gas phase behaviour obeys the ideal gas law,
- heat effects were neglected and the reactor is operated isothermally.

3.1. Particle model

Inside the particles the mass transfer is described using an effective pore diffusion model and the contribution of the adsorption and reaction rates is weighted according to the volume fractions of the corresponding functionalities in each local particle volume element resulting in the following expression for the particle mass balance (1):

$$\varepsilon_\mathrm{p}\frac{\partial c_{\mathrm{p},i}}{\partial t} = D_{\mathrm{eff},i}\left(\frac{\partial c_{\mathrm{p},i}}{\partial r}\frac{2}{r}+\frac{\partial^2 c_{\mathrm{p},i}}{\partial r^2}\right) - (1-\varepsilon_\mathrm{p})(f_{\mathrm{p,ads}}r_{\mathrm{V,ads},i} - f_{\mathrm{p,cat}}r_{\mathrm{V,cat},i}) \quad (1)$$

The boundary conditions for the particle mass balance are derived assuming a linear concentration profile in the particle boundary layer (2) and symmetric profiles within the particles (3)

$$k_{\mathrm{film},i}(c_i - c_{\mathrm{p},i}|_{r=R_\mathrm{p}}) = D_{\mathrm{eff},i}\left.\frac{\partial c_{\mathrm{p},i}}{\partial r}\right|_{r=R_\mathrm{p}} \quad (2)$$

$$\left.\frac{\partial c_i}{\partial r}\right|_{r=0} = 0 \quad (3)$$

'Conventional' particles consisting solely of adsorbent or catalyst can be described using the same model by simply setting the volume fraction of the corresponding functionality equal to 1.

3.2. Reactor model

The particles are incorporated in a fixed-bed reactor operated under the same conditions for multifunctional and conventional particles. A one-dimensional axial dispersion model is used to describe the reactor fluid bulk phase (4). The third term on the right-hand side of Eq. (4) accounts for the mass transfer from the fluid bulk phase to the particle surface, whereas in the case of the conventional benchmark adsorptive reactor the mass transfer to adsorbent and catalyst particles respectively, has to be distinguished by weighting the corresponding contribution according to the corresponding volume fractions of the particles in the fixed-bed (5)

$$\varepsilon\frac{\partial c_i}{\partial t} = -\left(u\frac{\partial c_i}{\partial x}+c_i\frac{\partial u}{\partial x}\right)+D_\mathrm{ax}\varepsilon\frac{\partial^2 c_i}{\partial x^2} - (1-\varepsilon)\frac{3}{R_\mathrm{p}}k_\mathrm{film}(c_i - c_{\mathrm{p},i}|_{R_\mathrm{p}}) \quad (4)$$

$$\varepsilon\frac{\partial c_i}{\partial t} = -\left(u\frac{\partial c_i}{\partial x} + c_i\frac{\partial u}{\partial x}\right) + D_{ax}\varepsilon\frac{\partial^2 c_i}{\partial x^2} - (1-\varepsilon)\frac{3}{R_P}(f_{x,ads}k_{film}(c_i - c_{p,ads,i}|R_P) + f_{x,cat}k_{film}(c_i - c_{p,cat,i}|_{R_P})) \quad (5)$$

Assuming the additivity of fluid volumes, the overall mass balance is derived by summing up all component mass balances (4) as follows (6):

$$\sum_i c_i\frac{\partial u}{\partial x} = \sum_i(1-\varepsilon)\frac{1}{V_P}\int_0^{R_P} r_{V,j}(r)(1-\varepsilon_p)4\pi r^2\,dr + \sum_i(1-\varepsilon)\frac{1}{V_p}\int_0^{R_P}\frac{\partial q_{i,ads}(r)}{\partial t}(1-\varepsilon_{p,ads})4\pi r^2\,dr \quad (6)$$

The reactor boundary conditions have been set assuming closed vessel behaviour [17]

$$u(c_i(x=0,t) - c_{0,i}) = D_{ax}\frac{\partial c_i(x=0,t)}{\partial x} \quad (7)$$

$$\frac{\partial c_i(x=L,t)}{\partial x} = 0 \quad (8)$$

At the outset of each reaction cycle the reactor contains an inert component

$$c_i(x,t=0) = 0, \qquad c_{p,i}(r,t=0) = 0 \quad (9)$$

3.3. Numerical solution

The model was implemented in Aspen Custom Modeler® with a modular model structure and solved using the method of lines. The spatial domain was discretised using fourth-order orthogonal collocation on 25 finite elements for the reactor length axis and on eight elements over the particle dimension, with the finite elements on the radial axis of the particle being allocated in such a manner so as to obtain an equivalent volume increment grid. This procedure ensured on one hand a meaningful comparison of particle configurations with different functionality arrangements, and on the other hand a better numerical resolution of the particle mass balances by using incremental control volumes of equal size [18].

3.4. Model parameters—test systems

Simulation studies were carried out for two test systems – the Claus process and water–gas shift reaction – in the first case a by-product is adsorbed and in the latter a reactant is desorbed, both resulting in a conversion enhancement of the equilibrium reaction according to Le Chatelier's principle. For the Claus process (10) the reaction kinetics over a γ-Al_2O_3-catalyst were described with a power law expression (11) [2]

$$2H_2S + SO_2 \rightleftharpoons \frac{3}{n}S_n + 2H_2O, \quad \Delta H_{ads} = -108\,kJ/mol \quad (10)$$

$$r_{V,i} = \nu_i(k_1 p_{H_2S} p_{SO_2}^{0.25} - k_2 p_{H_2O}) \quad (11)$$

and for the water–gas shift reaction (12) a Langmuir–Hinshelwood approach was used (13) [19]

$$CO + H_2O \rightleftharpoons H_2 + CO_2, \quad \Delta H_{ads} = -40.6\,kJ/mol \quad (12)$$

$$r_V = \frac{k(p_{CO}p_{H_2O} - p_{H_2}p_{CO_2}/K_{eq})}{(1+K_{CO}P_{CO}+K_{CO_2}p_{CO_2} + K_{H_2}p_{H_2} + K_{H_2O}p_{H_2O})^2} \quad (13)$$

In both cases water vapour was adsorbed on a 3A zeolite with the adsorption equilibrium being described using a Freundlich-type isotherm (14) [2]

$$q_{H_2O} = K_{F,H_2O}C_{H_2O}^{0.75}, \quad \Delta H_{ads} = -30.5\,kJ/mol \quad (14)$$

Table 1
Model parameters and correlations used in the case studies

	All systems		Claus process	Water–gas shift reaction
ε	0.4	d_p	4.92 mm [2]	3.5 mm
ε_p	0.5	L	1 m	0.5 m
T	250 °C	D	0.06 m	0.1
p	1.013 bar	u	0.02, . . ., 0.1 m/s	0.02, . . ., 0.1 m/s
D_i	Fuller, Schettler, Giddings, 1966	$f_{x,cat}$	0.43 [2]	0.5
k_{film}	Wakao, Funazkri, 1978			
D_{ax}	Wakao, 1984			

	Claus process	Water–gas shift reaction		
			H_2O in feed	No H_2O in feed
Reactor feed composition				
p_{H_2S}	0.1 bar	p_{CO}	0.058 bar	0.069 bar
p_{SO_2}	0.05 bar	p_{CO_2}	0.058 bar	0.069 bar
p_{N_2}	0.85 bar	p_{H_2}	0.714 bar	0.852 bar
		p_{H_2O}	0.17 bar	0.01 bar

The adsorption step was assumed to be instantaneous resulting in the following expression for the adsorption rate:

$$r_{V,ads,H_2O} = \frac{\partial q_{H_2O}}{\partial t} = \frac{\partial q_{H_2O}}{\partial c_{H_2O}} \frac{\partial c_{H_2O}}{\partial t} \quad (15)$$

The model parameters required were obtained from literature or calculated using empirical correlations as summarised in Table 1. In order to permit a consistent comparison of different particle configurations with one another and with a conventional adsorptive reactor, both the particle structure and the mass transfer characteristics have been averaged for adsorbent and catalyst and assumed to be independent of the distribution of the functionalities inside the multifunctional particles. In all cases the total adsorbent and catalyst fractions have been kept constant in order to study the mass transfer intensification independently.

Based on the parameter values reported in the literature, particle size and reaction rate were varied somewhat to investigate the influence of the ratio of reaction rate and internal diffusion as well as the ratio of convective and intra-particle mass transfer on the performance of multifunctional catalysts.

4. Simulation results and discussion

In order to be able to generalise the simulation results and compare the operating conditions for both test systems, two dimensionless numbers were used to characterise the system. The Thiele modulus (15), evaluated for the conditions at the inlet of a conventional adsorptive reactor, quantifies the highest ratio of reaction to the internal mass transfer rate that arises,

$$\Phi = \frac{R_p}{3} \sqrt{\frac{r_V(c_0)}{D_{eff} c_0}} \quad (16)$$

and the Stanton number for mass transfer (16), calculated assuming parabolic concentration profiles within the particle, expresses the ratio of the mass transfer rates for convection in axial direction to the diffusion from the bulk phase into the particle

$$St = \frac{3 k_{eff} L}{R_p u} \quad \text{with } k_{eff} = \left(\frac{1}{k_{film}} + \frac{R_p}{5 D_{eff}} \right)^{-1} \quad (17)$$

The reactor performance was quantified using the cycle time prior to the breakthrough point of unconverted reactant for a given reactor volume compared to a conventional adsorptive reactor operation.

For both test systems different multifunctional particle configurations were evaluated based on the relative cycle time enhancement in comparison to a conventional adsorptive reactor.

4.1. Claus process

The single stage Claus process, an adsorptive reactor concept proposed by Elsner et al. [2], was taken as a reference system for the potential application of multifunctional catalysts. In this example, the reaction cycle was terminated when a total sulphur conversion of 99.5% corresponding to current environmental standards was exceeded

$$X_{S,tot} = \frac{(c_{H_2S}(x = L) + c_{SO_2}(x = L))\dot{V}(x = L)}{(c_{H_2S}(x = 0) + c_{SO_2}(x = 0))\dot{V}(x = 0)} \leq 0.005 \quad (18)$$

For the standard reaction conditions (set 1 in Table 2) the application of multifunctional catalysts yielded only a slight improvement (7.5%) in the attainable reaction cycle time. Under the conditions chosen, the system exhibits hardly any mass transfer limitation ($\Phi = 0.45$) and thus the mass transfer intensification offered by multifunctional catalysts has no significant effect on the overall reactor performance. If intra-particle mass transfer limitations are more pronounced the performance enhancement with multifunctional catalysts improves dramatically (Table 2). Especially for lower Stanton numbers, i.e. longer characteristic diffusion times compared to the hydrodynamic residence times, the intensified mass transfer in multifunctional catalyst particles significantly reduces the bulk phase adsorbate concentration, which in turn results in less axial spreading of the breakthrough curve by convection (Fig. 4).

At higher Thiele modulus values the reaction zone inside the particles becomes restricted to an area in the vicinity of the surface (Fig. 3) and the core of the multifunctional particle is not utilised, thus diminishing the cycle time improvement compared to a conventional system. However, if the catalyst inside a multifunctional particle is distributed to give a higher activity towards the centre (structure D1 in Fig. 2) the reaction

Table 2
Summary of simulation results for the Claus process

Parameter set	Φ	St	$t_{cyc,conv.}$ (s)	Optimum particle structure[a]	$t_{cyc,opt}$ (s)	$\Delta t_{rel,opt}$ (%)	$(t_{cyc,opt} - t_{cyc,hom})/t_{cyc,hom}$ (%)
1	0.45	316.5	1397	C2	1502	7.5	0.8
2	0.8	174.9	1110	B2	1406	26.9	0.8
3a	2.6	174.9	1620	B1	1880	16.1	1.6
4a	2.6	41.3	1235	B1	2787	125.7	4.1
5	4.02	83.7	1215	C1	1502	23.6	3.6
6	12.96	18.6	1105	C1	2704	144.7	26.4

[a] See Fig. 2.

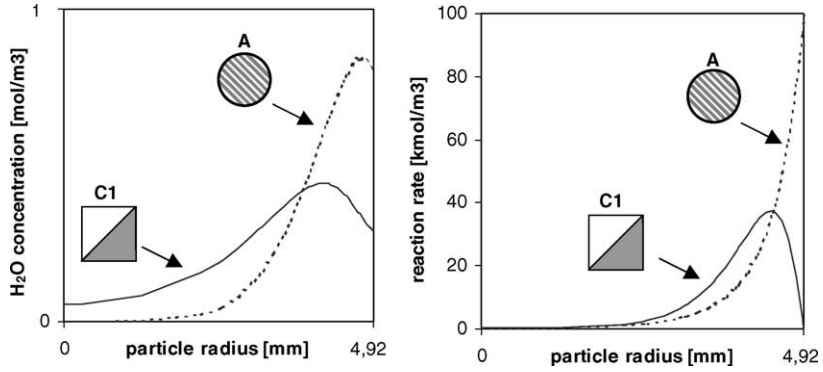

Fig. 3. Particle H_2O concentration and reaction rate profiles for Claus reaction, effect of catalyst distribution.

zone can be distributed more uniformly over the particle and thus both the particle utilisation and the cycle time can be improved (Fig. 3).

Generally the objective in optimising the particle structure is to achieve a maximum reaction rate while ensuring the compatibility of reaction and adsorption rates. Since the adsorption rate is always mass transfer limited this requires an integration of the two functionalities that is as intimate as possible. By varying the relative location of the catalyst the reaction rate can be influenced as described above for the case of fast reactions. It has to be noted that up to a Thiele modulus value of 4 the homogenous distribution of the functionalities exhibits nearly optimal performance (Table 2).

4.2. Water–gas shift reaction

For the water–gas shift reaction two different feed compositions were investigated—complete steam supply (no steam in feed) and make-up of steam consumption via desorption. In the first case the reaction mixture was already in chemical equilibrium upon entering the reactor and further reaction required water vapour desorption, while in the latter case the water vapour desorption had to precede the reaction. A minimum CO conversion of 90% was used as a criterion for the termination of the reaction cycle.

As was found for the Claus reaction, a considerable cycle time enhancement could be only obtained at lower Stanton numbers (Table 3). The low catalyst utilisation associated with the steep particle profiles occurring at high Thiele moduli could be compensated by arranging the catalyst inside a multifunctional particle in the same way as for the Claus reaction (Fig. 5). The two operation modes considered yielded basically similar results, whereas the effect of the mass transfer intensification is greater for the complete desorptive water vapour dosage, since the amount of water vapour desorbed is considerably larger. Thus it can be concluded that for a single equilibrium reaction the conversion enhancement by adsorptive product removal and desorptive reactant enrichment shows the same potential for performance enhancement using multifunctional catalysts and similar particle structures are found to be optimal.

4.3. Guidelines for the application of structured adsorptive catalysts

A significant advantage of multifunctional catalysts compared to the conventional adsorptive reactor configuration can be found only at low Stanton numbers, when moderate to strong mass transfer limitations prevail. The marginal gains for small particles and at high hydrodynamic residence times will in most cases not suffice to justify the increased expense and effort entailed in the preparation of more complex multifunctional catalysts. At elevated Thiele moduli a structured arrangement of the functionalities within the mul-

Table 3
Summary of simulation results for the water–gas shift reaction

Parameter set	Φ	St	$t_{cyc,conv.}$ (s)	Optimum structure[a]	$t_{cyc,opt.}$(s)	Δt_{rel} (%)
Desorptive resupply of H_2O (H_2O in reactor feed)						
1	1.17	294	1415	A	1445	2.1
2	2.13	95.6	1140	C1	1230	7.9
3	4.27	31	1223	C1	1500	22.6
4	8.54	7.1	1500	C1	1840	22.7
Complete desorptive supply of H_2O (no H_2O in reactor feed)						
1	1.17	423	2015	C1	2060	2.2
2	2.13	191	1858	C1	2030	9.3
3	4.27	55.5	1680	C1	2185	30.1
4	8.54	16.5	1160	C1	2130	83.6

[a] See Fig. 2.

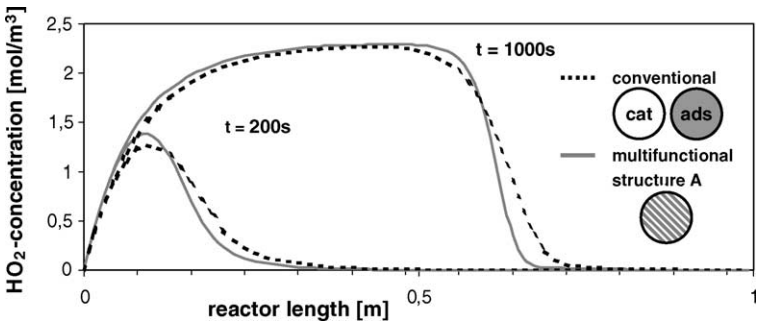

Fig. 4. Axial H_2O concentration profiles for Claus reaction.

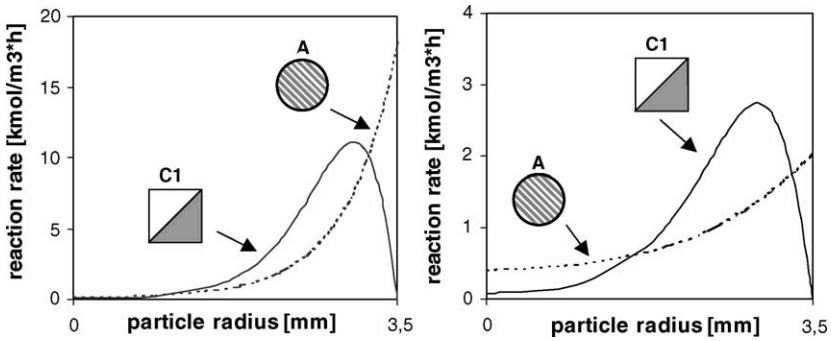

Fig. 5. Particle reaction rate profiles for water–gas shift reaction with (left) and without (right) H_2O in feed, effect of catalyst distribution.

tifunctional particles offers an additional improvement of the reactor performance through the deliberate manipulation of the intra-particle concentration profiles. Fig. 6 summarises the simulated cycle time improvements as a function of Thiele modulus and Stanton number, providing a rough guide as to the appropriate application window for multifunctional catalysts with integrated adsorption. Since the main advantage of multifunctional catalyst is found at low Stanton numbers this concept offers an effective means for the reduction of the residence times in adsorptive reactors, e.g. for reaction systems involving unstable components.

Based on the simulation results obtained in this study a simple design procedure valid for the conversion enhancement both by product-adsorption and reactant-desorption can be formulated (Fig. 7). A maximum degree of integration, i.e. maximum intensification of the mass transfer between the different functional sites, is obtained if the two functionalities are arranged as homogenously as possible, while the relative position of the catalyst volume fraction can be used to adapt the reaction and mass transfer rates. In multifunctional catalysts a given catalytic activity is distributed over a larger number of particles, which results in a lower average

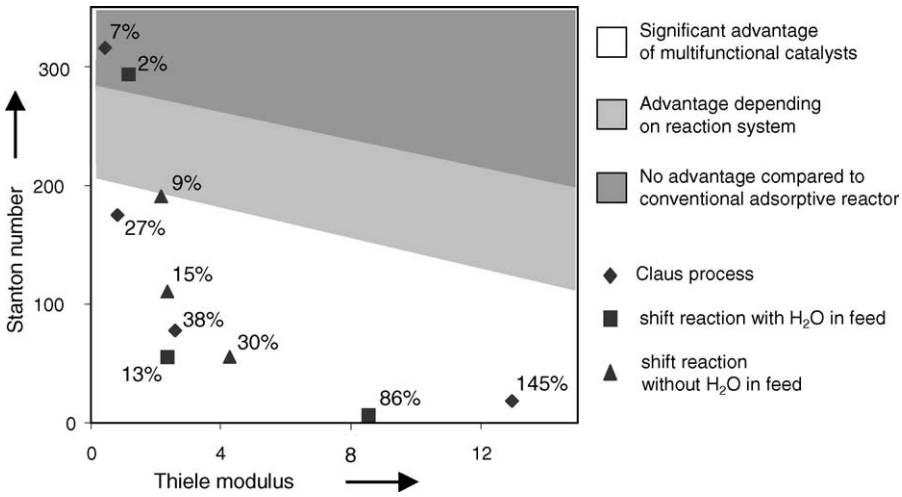

Fig. 6. Application window of multifunctional catalysts for the adsorptive conversion enhancement of equilibrium limited reactions.

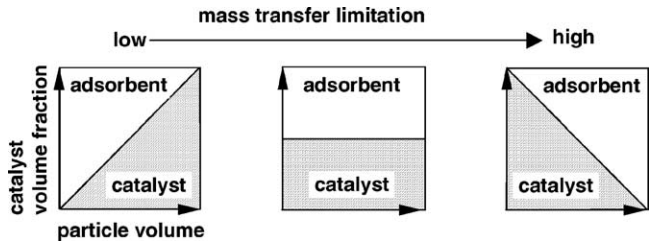

Fig. 7. Rules for the selection of the optimum structure of multifunctional catalysts with integrated adsorption sites.

activity per particle and less steep profiles compared to conventional "pure" catalyst particles. This dilution effect provides a better catalyst utilisation (higher effectiveness factor) and an increased overall reaction rate, especially for fast reactions. Furthermore, in a structured multifunctional particle poorly used catalyst could be replaced by adsorbent resulting in an increased adsorptive capacity and thus an extended cycle time.

5. Conclusions

The simulation results have demonstrated that multifunctional catalysts can serve as an appropriate tool for the circumvention of mass transfer limitations and thus offer an improved utilisation of both functionalities. The improved mass transfer between catalyst and adsorbent also allows an increase of the particle size or reduced residence times compared to a conventional adsorptive reactor design. The compatibility of adsorption and reaction rates, which is a crucial criterion for the feasibility of adsorptive reactors [4], is facilitated by multifunctional catalysts and thus the operating window for adsorptive reactors can be augmented by their use. The selection of the optimal structure of multifunctional adsorptive catalysts according to Fig. 7 is straightforward and involves only three different structural variants.

However, if the mass transfer between the different functionalities is not limiting, the benefit of multifunctional catalysts will be not adequate to justify the more complex manufacturing process. Since the presented model assumes isothermal conditions, which is realistic only for systems involving low concentrations and heats of reaction as in the two case studies discussed above, further investigations based on an extended model are required to cover thermal effects occurring in multifunctional catalyst particles for concentrated reaction systems with high heats of reaction. The performance enhancement found for a single reversible reaction suggests similar or even greater improvements for more complex reaction schemes, e.g. increased selectivity for consecutive side-reactions, and holds promise for further investigations of multifunctional catalysts with integrated adsorption sites. The macrostructuring of multifunctional catalyst particles along the length of a fixed-bed, to provide locally optimised distributions of the functionalities within the particles, together with chronological variation of operating parameters, such as pressure, during the course of the reaction cycle can be exploited to expand the horizons of the technique and further enhance performance through additional degrees of freedom in process design. For more complex non-linear adsorption and reaction kinetics and equilibria one might expect advantages from intra-particle concentration profile manipulation above and beyond those resulting from simple mass transfer intensification.

References

[1] D.W. Agar, Chem. Eng. Sci. 54 (1999) 1299–1305.
[2] M.P. Elsner, C. Dittrich, D.W. Agar, Chem. Eng. Sci. 57 (2002) 1607–1619.
[3] Y. Ding, E. Alpay, Chem. Eng. Sci. 55 (2000) 3929–3940.
[4] J.R. Hufton, S. Mayorga, S. Sircar, AIChE J. 45 (1999) 248–256.
[5] C. Han, D.P. Harrison, Chem. Eng. Sci. 49 (1994) 5875–5883.
[6] M. Kuczynski, et al., Chem. Eng. Sci. 42 (1987) 1887–1898.
[7] A. Kruglov, Chem. Eng. Sci. 49 (1994) 4699–4716.
[8] S. Goto, T. Tagawa, T. Oomiya, Chem. Eng. Essay 19 (1993) 978–983.
[9] I. Yonsunthon, E. Alpay, Chem. Eng. Sci. 54 (1999) 2647–2657.
[10] G.H. Xiu, P. Li, A.E. Rodrigues, Chem. Eng. Sci. 58 (2003) 3425–3437.
[11] D.J. Gunn, W.J. Thomas, Chem. Eng. Sci. 20 (1965) 89–100.
[12] D.R. Rutkin, E.E. Petersen, Chem. Eng. Sci. 34 (1979) 109–116.
[13] M. Kawase, et al., Chem. Eng. Sci. 51 (1996) 199–209.
[14] V.M. Silva, A.E. Rodrigues, AIChE J. 48 (2002) 625–634.
[15] M. Morbidelli, A. Gavriilidis, A. Varma, Catalyst Design, Cambridge University Press, 2001.
[16] D.R. Ardiles, O.A. Scelza, A.A. Castro, Coll. Czechoslov. Chem. Commun. 50 (1985) 726–737.
[17] P.V. Danckwerts, Chem. Eng. Sci. 2 (1953) 1–13.
[18] S. Crone, Dissertation, Universität Dortmund, 2002.
[19] N.E. Amadeo, M.A. Laborde, Int. J. Hydrogen Energy 20 (1995) 949–956.